Journal of Materials Chemistry B

Accepted Manuscript

This article can be cited before page numbers have been issued, to do this please use: X. Xi, S. Hu, Z. zhou, X. Liu, J. Tang and Y. Shen, *J. Mater. Chem. B*, 2016, DOI: 10.1039/C6TB01597B.

ROYAL SOCIETY OF CHEMISTRY

www.rsc.org/materialsB

View Article Online
DOI: 10.1039/C6TB01597B

Journal of Materials Chemistry B

ARTICLE

Dendrimers with protocatechuic acid building blocks for anticancer drug delivery

Received 00th January 20xx,
Accepted 00th January 20xx

DOI: 10.1039/x0xx00000x

www.rsc.org/

Xiujuan Xi†, Shiqi Hu†, Zhuxian Zhou*, Xiangrui Liu, Jianbin Tang, Youqing Shen*

Protocatechuic acid (3,4-dihydroxybenzoic acid; PCA) is a well-known antioxidant compound and a potential antitumor drug that is commonly found in fruits and vegetables. This article describes the development of novel biodegradable dendrimers that contain PCA as building blocks. The structures of the dendrimers were characterized by nuclear magnetic resonance, gel permeation chromatography, and matrix-assisted laser-desorption ionization time-of-flight mass spectrometry. PCA dendrimers could serve as potential anticancer drugs and also as nanocarriers for anticancer drug delivery. PCA dendrimers can easily be loaded with hydrophobic drugs such as doxorubicin that benefit from the binding interaction between PCA and the drug. Doxorubicin-loaded PCA dendrimers exhibited pH and redox-dual responsive drug release in vitro. The antitumor effect of PCA dendrimers to which polyethylene glycol polymer chains have been attached and doxorubicin-loaded dendrimers was preliminary evaluated both *in vitro* and *in vivo*.

Introduction

Dendrimers are nanosized, highly branched macromolecules characterized by well-defined monodisperse structures, internal cavities for guest molecule encapsulations, ample surface groups for functionalization, and an unusually low intrinsic viscosity that allows easy transport in the blood.[1, 2] These distinctive characteristics make dendrimers ideal nanocarriers for drug and gene delivery because they allow for control over the molecular weight, hydrophilicity, multiplicity of therapeutic drugs, anchoring with specific active targeting agents, and pharmacokinetic behavior.[3-5]

Of the many available dendrimers, poly(amidoamine) (PAMAM) dendrimers are the most widely studied for drug and gene delivery.[6, 7] However, amine-terminated PAMAM dendrimers are not biodegradable *in vivo* and are positively charged on the surface, and they interact nonspecifically with negatively charged biological membranes and cause a variety of problems in *in vivo* applications, including cytotoxicity, hemolytic toxicity, rapid clearance from the blood circulation, and a high level of uptake in the reticuloendothelial system.[8] These problems have hindered their clinical application. As a result, efforts have focused on reducing the toxicity and improving the pharmacokinetic behavior by developing biodegradable and biocompatible dendrimers such as polyester dendrimers,[9, 10] polylysine dendrimers,[11] and polyether dendrimers.[12] Polyester dendrimers are most attractive because of their good biodegradability, which facilitates dendrimer clearance by the hydrolysis of macromolecules into small molecules.[10, 13, 14] However, these dendrimers are typically inert, and their degradation products have no effect on the treatment of tumors or other diseases, so the carrier must be excreted in the form of additional waste, thus increasing the physical exertion required of cancer patients.

In this paper, we propose that the use of a bioactive molecule as the building blocks of a polyester dendrimer would minimize the use of other inert materials and increase the bioactivity of the nanocarrier. Protocatechuic acid (3,4-dihydroxybenzoic acid; PCA), a phenolic compound isolated from plants, fruits, nuts, and black rice; has demonstrated antioxidant, antibacterial, and antitumor promotion effects. It has been reported that PCA may prevent tumorigenesis[15] and inhibit the proliferation and metastasis of a series of cancer cells.[16] PCA includes one carboxyl group and two phenolic hydroxyl groups, and thus can be used as an AB2-type building block for the preparation of polyester dendrimers with a double-stage convergent approach. PCA dendrimers are designed to hydrolyze under physiological conditions, and the unique biological properties of the PCA compound may endow PCA dendrimers with antitumor activity. Furthermore, PCA can also serve as a drug-binding molecule because of its high π-π stacking binding interaction with benzene-containing therapeutic drugs such as doxorubicin (DOX).[17, 18] The strong interaction of the dendrimers with DOX may facilitate drug loading and reduce the initial drug release in systemic administration. The antitumor activity of PEGylated PCA dendrimers (PCA4-PEG) and DOX-loaded PCA dendrimers (PCA4-PEG/DOX) was preliminary evaluated *in vitro* and *in vivo*.

Experimental

Materials

Reagent-grade dichloromethane (DCM) and tetrahydrofuran (THF) were predried over calcium hydride (CaH_2) and distilled under argon immediately before use. DMF was distilled from CaH_2 just before

Center for Bionanoengineering and State Key Laboratory for Chemical Engineering, Department of Chemical and Biological Engineering, Zhejiang University, Hangzhou 310027, China. Email: zhouzx@zju.edu.cn or shenyq@zju.edu.cn

† Equal contributor. Electronic Supplementary Information (ESI) available: [details of any supplementary information available should be included here]. See DOI: 10.1039/x0xx00000x

View Article Online
DOI: 10.1039/C6TB01597B

use. All other solvents and chemicals were used as received. DOX hydrochloride salt (DOX·HCl) was supplied by Zhejiang Hisun Pharmaceutical Co. (Taizhou, China). PCA, *tert*-butyldimethylsilyl chloride, (4-chlorocarbonylphenyl) boronic anhydride , tetrabutylammonium fluoride (TBAF), glutathione (GSH), and PEG2000 were obtained from Aladdin Chemistry Co. (Shanghai, China).

Instruments

Nuclear magnetic resonance (^{1}H NMR) spectra were recorded with a Bruker Avance DRX-400 spectrometer (Bruker BioSpin Corporation, Billerica, MA) with deuterated chloroform ($CDCl_3$) or dimethyl sulfoxide (DMSO-d_6) as a solvent and tetramethylsilane as the internal standard. All chemical shifts are reported in parts per million (δ, ppm). Gel permeation chromatography (GPC) was performed on a Wyatt GPC/SEC-MALS (Wyatt Technology Corp., Santa Barbara, CA) system equipped with a DAWN® HELEOS® II 18-angle static light scattering detector and an Optilab® T-rEX™ refractive index detector, and a pair of Shodex KF-402.5 HQ and KF-404 HQ columns at 30 °C using THF as the eluent at a flow rate of 0.80 ml/min. Data were recorded and processed with ASTRA v6.0 (Wyatt Technology Corp.) software. Matrix-assisted laser-desorption ionization time-of-flight mass spectrometry (MALDI-TOF MS) were recorded on a Bruker ultrafleXtreme™ MALDI-TOF MS (Bruker Daltonics GmbH, Bremen, Germany) using α-cyano-4-hydroxycinnamic acid diethylammonium (CCA) as the matrix. One microliter of dendrimer solution (1×10^{-2} M PCA, methanol) was mixed with 50 µL of matrix solution (10 gL^{-1} CCA, methanol). One microliter of the mixture was deposited onto the sample stage and allowed to dry in air. The laser intensity was set to the lowest value possible to acquire high-resolution spectra. The spectra were analyzed with FlexAnalysis v3.4 (Bruker Daltonics GmbH, Bremen, Germany).

Synthesis of 3,4-bis(*tert*-butyldimethylsiloxy) benzoic acid (2)

PCA (15.4 g, 100 mmol) and imidazole (56.0 g, 800 mmol) was dissolved in DMF (150 ml) and cooled to 0 °C. To this solution, *tert*-butylchlorodimethylsilane (60.3 g, 400 mmol) in DMF (300 ml) was slowly added under N_2. The temperature of the solution was allowed to increase to room temperature (RT) and the mixture was stirred overnight. The reaction mixture was then poured into saturated aqueous $NaHCO_3$ (500 ml), extracted with ether, and washed with brine. The combined organic extract was dried over anhydrous Na_2SO_4 and concentrated on a rotary evaporator.

The concentrate was then dissolved in a mixed solvent of THF (80 ml) and MeOH (240 ml). To this solution, an aqueous solution of K_2CO_3 (0.72 M, 80 ml) was added, and the mixture was stirred at RT for 2 h. The reaction mixture was then concentrated to a 1/4 volume and diluted with brine (200 ml). The pH of the solution was adjusted to 4-5 with $KHSO_4$ (1.0 M), and the resulting mixture was extracted with ether. The organic extract was combined, washed with brine, dried over anhydrous Na_2SO_4, filtered and rotary evaporated to dryness to give 2 as a white powdery substance (30 g) at a 78% yield.[19] ^{1}H NMR (400 MHz, $CDCl_3$, 25°C): δ (ppm) 12.11 (br s, 1H, COO*H*), 7.66-7.64 (dd, 1H, 6-H of PCA), 7.61 (d, 1H, 5-H of PCA), 6.89 (d, 1H, 2-H of PCA), 1.01 (d, 18H, $ArOSi(Me)_2C(CH_3)_3$), 0.26 (d, 12H, $ArOSi(CH_3)_2$ tBu) (Supporting information, Figure S2).

Synthesis of 3,4-bis(*tert*-butyldimethylsiloxy)benzoyl chloride (3)

A suspension of 3,4-bis(*tert*-butyldimethylsiloxy) benzoic acid (2) (20 g, 52 mmol) in a mixture solvent of toluene (120 ml) and DMF (0.2 ml) was stirred at RT. Thionyl chloride (12 ml, 165 mmol) dissolved in toluene (15 ml) was added dropwise into the previous solution over 10 min. The mixture was stirred at RT for 20 min and then heated to 50°C and stirred for another hour until gas evolution had ceased. The yellow solution was evaporated, and the residue was taken up in 20 ml of toluene at 70 °C. The product was dissolved, and the yellow, viscous side product remained undissolved. The product solution was decanted and precipitated by adding 55 ml of cyclohexane to the hot toluene solution and separated to give a yellowish oil at a 86% yield (18 g)[20].

Synthesis of methyl protocatechuate (4)

The synthesis of methyl protocatechuate was adapted from the work of Alam et al.[21] a PCA (9.0 g, 58 mmol) was dissolved in dry methanol (150 ml), to which a catalytic amount (0.3 ml) of concentrated sulfuric acid was carefully added. The solution was heated under reflux for 24 h at 65 °C and then cooled to RT. To this solution, sodium hydroxide (2.0 M) was added dropwise until the excess acid had been neutralized. The solvent was removed using a rotary evaporator to yield crude methyl protocatechuate as a white crystalline solid. To separate the methyl protocatechuate from any unreacted PCA impurities, the product was dissolved in a mixture of ethyl acetate (60 ml) and pure water (20 ml). The organic layer containing the methyl protocatechuate was separated, further washed with pure water (2 × 20 ml) and brine (40 ml), and then dried over anhydrous $MgSO_4$. The solvent was removed under vacuum, and the product was recrystallized from hot water, filtered and dried on a high vacuum line to give methyl protocatechuate (8.9 g; 91%) as a white crystalline solid, ^{1}H NMR (400 MHz; DMSO-d_6, 25 °C): δ (ppm) 9.53 (br s, 2H, 3-O*H*), 7.32 (d, 1H, 5-H of PCA), 7.29-7.27 (dd, 1H, 6-H of PCA), 6.78 (d, 1H, 2-H of PCA), 3.73 (3H, s, $-CO_2CH_3$) (Figure S2).

Synthesis of protocatechuic acid tert-butyldimethylsilyl ether dendrimers (PCAn-TBDMS) and protocatechuic acid dendrimers (PCAn-OH)

Methyl protocatechuate (4) (1.0 g, 6.0 mmol) and triethylamine (2.6 ml; 18.68 mmol) were dissolved in dry THF (20 ml) and stirred at RT. To this solution, 3,4-bis(*tert*-butyldimethylsiloxy)benzoyl chloride (3) (7.2 g, 18 mmol) in 10 ml of THF was slowly added under N_2 at 0°C. The solution was allowed to warm to RT and was stirred overnight. The reaction mixture was filtered to remove insoluble fraction, and the filtrate was concentrated by rotary evaporation. The product was purified by column chromatography (SiO_2, hexane/ethyl acetate 10:1, R_f = 0.5) to give PCA1-TBDMS as a white powdery substance (4.2 g) at a 78% yield. ^{1}H NMR (400 MHz, $CDCl_3$, 25 °C): δ (ppm) 8.0 (d, 2H, Ar-*H*), 7.59-7.48 (m, 5H, Ar-*H*), 3.88 (s, 3H, $-CO_2CH_3$), 0.94 (d, 36H $-OSi(Me)_2C(CH_3)_3$), 0.22 (s, 12H, $-OSi(CH_3)_2$ t-Bu), 0.13 (d, 12H, $-OSi(CH_3)_2$ t-Bu).

TBAF (7.07 g, 26.92 mmol) was added to a dry THF solution (20 ml) of PCA1-TBDMS (4 g, 4.4 mmol) under N_2 at 0 °C, and the mixture was stirred at 0 °C overnight. The reaction mixture was then poured into saturated aqueous NH_4Cl (50 ml) and extracted with ethyl acetate. The combined organic extract was washed with brine, filtered, and dried over anhydrous Na_2SO_4. The solution was concentrated by rotary evaporation, and the residue was poured into DCM to precipitate the crude product. The product was purified by dissolving in methanol (2 ml) and precipitating in DCM. The purified product was dried in a vacuum oven to give PCA1-OH as a white powdery substance (1.96 g) at a 100% yield. MALDI-TOF (CCA as matrix, *m/z*, $[M+Na]^+$) 463.47 (obsd), 463.06 (calcd for $C_{22}H_{16}O_{10}Na$). ^{1}H NMR (400 MHz, DMSO-d_6, 25 °C): δ (ppm) 9.78 (br s, 4H, -O*H*), 7.96 (d, 2H, Ar-*H*), 7.60 (d, 1H, Ar-*H*), 7.38 (s, 2H, Ar-*H*),

View Article Online
DOI: 10.1039/C6TB01597B

7.35 (d, 2H, Ar-*H*), 6.77 (dd, 2H, Ar-*H*), 3.88 (s, 3H, -CO_2CH_3). PCA2-OH, PCA3-OH, PCA4-OH and PCA5-OH were synthesized by repeating the reaction with 3 and followed by deprotection in TBAF solution.

PEGylation of PCA4-OH dendrimer

The synthesis of PCA4-OH PEG derivatives is summarized in Scheme S1. A solution of MPEG (2KDa, 5 g, 2.5 mmol) and triethylamine (0.7 ml) in 30 ml of DCM was added to the solution of (4-chlorocarbonylphenyl)boronic anhydride (0.9 g, 5 mmol) in 15 ml of DCM, and the mixture was stirred at RT for 6 h. The insoluble fraction was filtered, and the filtrate was concentrated with a rotary evaporator. The residual solution was dropped in cold diethyl ether to precipitate the crude product. The crude product was purified by dissolving in DCM and precipitating from cold diethyl ether. The purified product was dried in a vacuum to give PEG-B-OH as a white powdery substance (4.67g) at a 86% yield. ^{1}H NMR analysis indicates that 75% of the end groups were modified with phenylboronic acid (Figure S2 and S3). PEG-B-OH (2 eq. mol) and PCA4-OH (1eq. mol) was dissolved in dry THF with anhydrous Na_2SO_4. The mixture was stirred at RT for 3 h and filtered, and the filtrate was precipitated in cold ether, filtered, and dried in vacuum to obtain PCA4-PEG (Figure S3), ^{1}H NMR analysis shows that 85% of the dendrimer end groups were modified with PEG.

Determination of molecular weights by ^{1}H NMR spectra

Two peaks of protons (a and b) with no overlap with any other peaks were chosen for calculating and evaluating the molecular weights of dendrimers. From the integral ratio of protons a and b in ^{1}H NMR (χ_{NMR}) and the ratio of the number of the protons in the theoretical dendrimer structure (χ_T), the molecular weight of dendrimers can be determined according to:

$$\boldsymbol{Wt(NMR)} = \frac{\chi_{NMR}}{\chi_T} \cdot \boldsymbol{Wt} = \frac{\frac{S_a}{S_b}}{\frac{\Sigma H_a}{\Sigma H_b}} \cdot \boldsymbol{Wt} \quad \text{(Equation 1)}$$

where χ_{NMR} is the integral ratio of protons (a) and (b) in ^{1}H NMR, χ_T is the ratio of the number of protons in the theoretical dendrimer structures, S_a and S_b are the peak areas of protons at a and b positions, ΣH_a and ΣH_b are the sums of protons at the a and b positions in the molecular formula of the PAn-TBDMS dendrimer, and *Wt* is the theoretical molecular weight of the dendrimers.

Preparation of DOX-loaded dendrimer

The DOX-loaded dendrimer was prepared as follows. Briefly, DOX·HCl (5 mg) was dissolved in 1 ml of DMSO. Triethylamine (20 µl) was added to the solution, and the mixture was stirred at RT overnight. PCA4-PEG (30 mg) was added to the previous solution, and the mixture was stirred for 30 min. Distilled water (9 ml) was then dropped into the solution. The mixture was stirred at RT for another 30 min and dialyzed (molecular weight cutoff, 3500 Da) against pure water for 10 h (2 L × 3). The DOX content was determined by measuring its UV-Vis absorbance at 480 nm and calculated according to a calibrated linear curve of standard DOX solutions.

The drug encapsulation efficiency (EE) and the drug loading content (DLC) were calculated with the following formulas:

$$\boldsymbol{EE}(\%) = \frac{\boldsymbol{mass\ of\ drug\ entrapped}}{\boldsymbol{mass\ of\ feed\ drug}} \times \mathbf{100}$$

$$\boldsymbol{DLC}(\%) = \frac{\boldsymbol{mass\ of\ drug\ entrapped}}{\boldsymbol{mass\ of\ nanoparticle}} \times \mathbf{100}$$

The sizes (hydrodynamic diameters) and zeta potential of the dendrimers were determined with a Nano-ZS Zetasizer (Malvern Instruments Ltd., UK). Each measurement was performed in triplicate, and the results were processed with DTS software version 6.20.

In vitro hydrolysis and drug release

The degradation of PCA1-OH was studied by culturing PCA1-OH with dithiothreitol (DTT, 10 mM) and triethylamine (TEA, 1 mM). At different time interval, the solution was sampled for ^{1}H NMR analysis. The release of DOX from the DOX-loaded dendrimers was studied with a dialysis method. DOX-loaded dendrimers (DOX, 400 µg/ml) were loaded into a dialysis bag (molecular weight cutoff, 3500 Da) and immersed in 200 ml of HEPES buffer (0.01 M, pH 7.4) with or without 10 mM of GSH or HEPES buffer (0.01 M, pH 5.5) at 37 °C with constant shaking. At timed intervals, the UV-Vis absorbance at 480 nm of the liquid in dialysis bags was measured to determine the DOX concentration.

Cell culture

A549 human lung cancer cells, BCap37 human breast cancer cells, and HepG2 liver cancer cells were obtained from the American Type Culture Collection (Manassas, VA). All cell lines were maintained in RPMI 1640 (Gibco) supplemented with 10% heat-inactivated fetal bovine serum (Gibco), penicillin (100 units/ml), and streptomycin (100 µg/ml) in a humidified atmosphere of 5% CO_2 at 37 °C.

Cellular uptake and intracellular distribution

A549 cancer cells were seeded onto glass-bottom petri dishes (MatTek, Ashland, MA, USA, no. P35G-1.0-14-C) at a density of 100,000 cells per dish in 1 ml of medium and incubated for 24 h before treatment. Cells were incubated with free DOX or DOX-loaded dendrimer at a DOX-equivalent dose of 2 µg/ml. LysoTracker (Molecular Probes, Carlsbad, CA) was added to each dish at a concentration of 200 nM 2 h before observation. DAPI (2-(4-amidinophenyl)-6-indolecarbamidine; Beyotime, China) was added to each dish at a concentration of 0.5 µg/ml 15 minutes before observation. The cells were then thoroughly washed three times with PBS; the images were taken at different times using a confocal laser scanning microscope (CLSM, Nikon-A1 system, Japan). Nuclear staining was observed with a 405-nm laser; the emission wavelength was 425 to 475 nm and appeared blue. LysoTracker was observed using a 488-nm laser; the emission wavelength was 510 to 540 nm and appeared green. The DOX-loaded dendrimer was observed using a 543-nm laser; the emission wavelength was 560 to 610 nm and appeared red. Images were taken by using the lasers sequentially with a 60× objective lens.

***In vitro* cytotoxicity**

The cytotoxicity of the DOX-loaded dendrimer was determined by (3-(4,5-dimethylthiazol-2-yl)-2,5-diphenyltetrazolium bromide) MTT assay. Briefly, cells (4000 cells per well) were evenly seeded onto 96-well plates and incubated overnight. The cells were incubated with serial dilutions of free DOX, PCA4-PEG/DOX, and blank carriers PCA4-PEG for 48 h. After treatment, the cells were incubated with fresh medium containing 0.75 mg/ml of MTT for 3 h, which allowed viable cells to reduce the yellow tetrazolium salt (MTT) into dark blue formazan crystals. Finally, DMSO was added to dissolve the formazan crystals. The absorbance at 562 nm was recorded with a reference filter of 620 nm, using a microplate spectrophotometer (SpectraMax M2e, Molecular Devices, Sunnyvale, CA). Each drug concentration was tested in triplicate and in three independent experiments.

View Article Online
DOI: 10.1039/C6TB01597B

In vivo antitumor effect

Female BALB/c homozygous athymic nude mice (6 to 8 weeks of age) were purchased from the Animal Center of Zhejiang University and maintained under standard conditions. The experimental procedures were approved by the Animal Ethics Committee of Zhejiang University and were carried out in accordance with institutional guidelines.

The *in vivo* antitumor efficacy of the drug-loaded dendrimers was examined in nude mice with subcutaneous human lung carcinoma (A549). Athymic nude mice were inoculated by the subcutaneous injection of A549 cells (5×10^6) in the left auxiliary flank. The tumor volume of each mouse was determined by measuring two dimensions with calipers and calculated according to the formula $V = 1/2\ ab^2$, wherein V is the volume of the tumor, a is the longest diameter of the tumor, and b is the shortest diameter of the tumor. When the tumors reached an average volume of approximately 80 to 150 mm^3, the mice were randomly divided into their experimental groups (eight per group): (1) PBS (negative control group), (2) PCA4-PEG, (3) PCA4-PEG/DOX, and (4) free DOX. The DOX formulations were given by intravenous injection into the tail vein in five doses of 4 mg/kg once every 3 days. Throughout the study, the mice were weighed and their tumors were measured with calipers. At the end of the experiments, all animals were sacrificed according to institutional guidelines. The tumors were resected, weighed, and fixed in formalin for paraffin embedding. The tumor inhibition rate (TIR) was calculated with the following equation: TIR = 100% × (mean tumor weight of control group − mean tumor weight of experimental group)/mean tumor weight of control group.

Histological examination of tumor tissues

Tumor and other tissue samples were fixed with 4% neutral buffered paraformaldehyde, embedded in paraffin, and cross-sectioned at a thickness of 5 μm. The sections were prepared and stained with hematoxylin and eosin (Fisher Scientific, Waltham, MA) for histologic examination and examined with light microscopy.

Statistical analysis

The data are presented as means ± standard errors. Tumor volumes over time were analyzed by one-way analysis of variance and then by Student's *t*-test. All other statistical analyses were performed using Student's *t*-test. Differences were considered to be statistically significant at a level of $p < 0.05$.

Results and discussion

Synthesis and characterization of DOX-loaded protocatechuate (PCA) dendrimers

PCA dendrimers were synthesized following the procedure as shown in Scheme 1. To synthesize dendrimers with PCA as the building blocks, we designed a pair of PCA-derived monomers, 3,4-bis(tert-butyldimethylsiloxy)benzoyl chloride (3) as the repeating units and methyl protocatechuate (4) as the dendrimer core. In the propagation step, one molecule of 4 was reacted with two molecules of 3 by the reaction of hydroxyl groups and acyl chloride to form biodegradable ester bonds. The TBDMS-protected hydroxyl groups were deprotected with TBAF. Repeating these two steps produced PCA dendrimers with different generations.

The molecular weight and structure of the PCA dendrimers was characterized by GPC, ^{1}H NMR, ^{13}C NMR, and MALDI-TOF mass spectra. All of the dendrimers showed monomodal molecular weight distribution, as indicated by GPC traces (Figure 1). The GPC traces of PCAn-TBDMS gradually shifted to the high–molecular-weight region with the increase of dendrimer generations, and no trace of low–molecular-weight fragments were found, which indicates complete coupling and successful purification of each step.

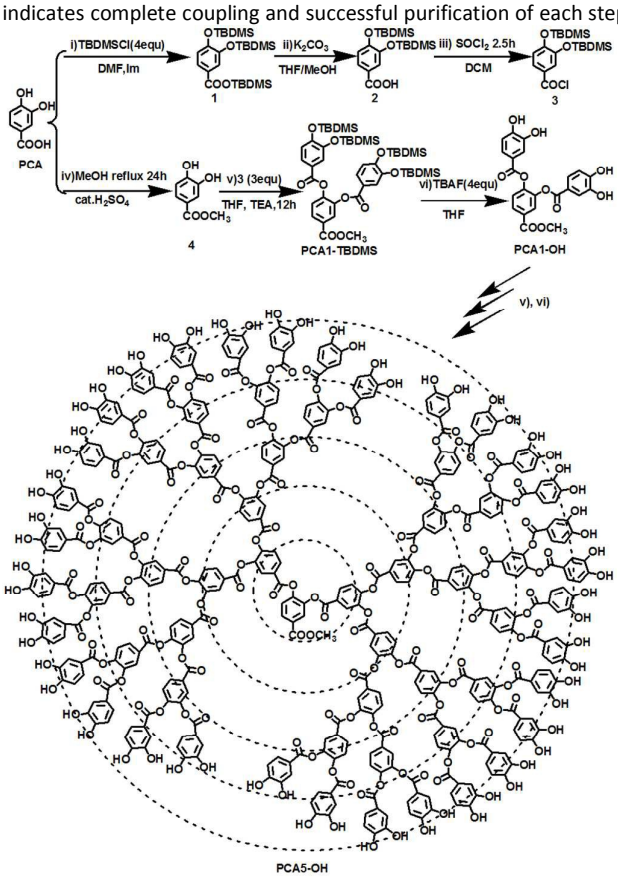

Scheme 1. Synthesis of PCA dendrimers.

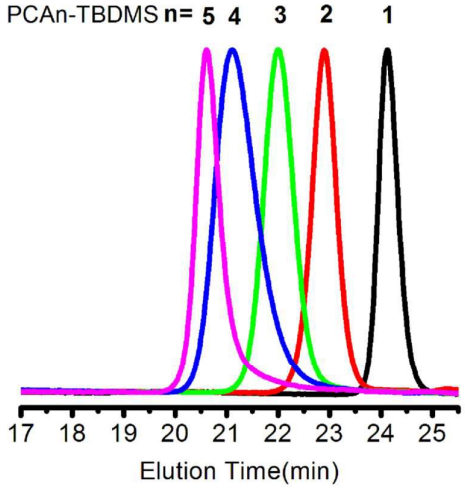

Figure 1. GPC traces (THF, 30 °C, 0.8 ml/min) of PCAn-TBDMS (n = 1-5).

Moreover, the polydispersity of the dendrimers are mostly close to 1.00 in the range from 1.02 to 1.14, which indicates that the obtained dendrimers have few defects and are of high purity. The relative molecular weights of PCAn-TBDMS measured by GPC were

View Article Online
DOI: 10.1039/C6TB01597B

Table 1. Theoretical molecular weights (Mw(T)) and experimental measurements of PCAn-TBDMS (n = 1-5) determined by GPC, ^{1}H NMR, and MALDI-TOF MS.

PCA dendrimers	Mw(T)	Mn (GPC)	Mw/Mn (GPC)	Mw (NMR)	*m/z*[M+Na]$^+$ (MALDI-TOF) [a]
PCA1-TBDMS	879.4	734	1.02	879	919.6 [M+K]$^+$
PCA2-TBDMS	1898.8	1860	1.03	1925	1920.8
PCA3-TBDMS	3901.8	3460	1.06	3821	3925.5
PCA4-TBDMS	7907.6	5870	1.14	7798	7937.8
PCA5-TBDMS	15915.6	8740	1.10	15722	16006.6

[a] PCAn-TBDMS dendrimers with high generations are not stable at high laser intensity; number represents found peak of undecomposed fraction.

calculated according to polystyrene standards, which are lower than the theoretical molecular weights, especially for dendrimers of high generation (Table 1), because dendrimers exhibit a lower hydrodynamic volume than their linear homologues due to theircompact architecture.[22, 23] The chemical structures of synthesized PCAn-TBDMS dendrimers were further confirmed by ^{1}H NMR as shown in Figure 2A. Peaks on ^{1}H NMR spectra of PCAn-TBDMS dendrimers become broader as the dendrimer generation increased, which is attributed to the densely packed structure of the dendrimer arising from the AB2 substitution pattern and the high tert-butyldimethylsilyl ether density generated at the periphery. The ^{1}H NMR spectra of the dendrimers can accurately indicate protons at specific positions in the structure and can also be used to determine molecular weight.[24] The molecular weight of PCAn-TBDMS can be calculated from the ^{1}H NMR spectra from the integration ratio of the peaks around 3.8 ppm (peak a, -$COOCH_3$, dendrimer core) and 0.9 ppm (peak b, -Si-$C(CH)_3$, TBDMS) according to Equation 1 in experimental section (Figure 2B). As the dendrimer generation increased from G1 (PCA1-TBDMS) to G5 (PCA5-TBDMS), the ratio of b:a increased from 36:3 to 569:3 and the calculated Mw(NMR) increased from 879 Da to 15722 Da (Table 1). All of the molecular weights calculated from the ^{1}H NMR spectra are very close to their theoretical values, with less than 2% error. This further confirmed the successful synthesis of PCAn-TBDMS dendrimers. The structures of the PCAn-TBDMS dendrimers were further studied with MALDI-TOF MS (Figure S4). A product peak with a molecular weight close to the theoretical value was found on each spectrum. However, careful MS analysis revealed that the degradation of phenol ester occurred upon ionization during MALDI analysis and resulted in multiple peaks with molecular weight differences (Δm/z) of 250 Da in the MS.[25]

Hydroxyl terminated PCA dendrimers were obtained after the deprotection of TBDMS by TBAF. The disappearance of TBAF peaks between 0 and 1 ppm on the ^{1}H NMR spectra indicated successful deprotection (Figure 3), and the structure was further confirmed by ^{13}C NMR (Figure S5). Product peaks of PCAn dendrimers with molecular weights close to the theoretical values were also identified in the mass spectra, accompanied by multiple decomposed fragments (Figure S6). The fourth generation of PCA dendrimer PCA4-OH was chosen for PEGylation and used as a carrier for delivery of the anticancer drug DOX. PEGylation endows nanocarriers with many favorable properties that include reduced reticuloendothelial system clearance and prolonged blood circulation time by avoiding protein opsonization.[26-28]

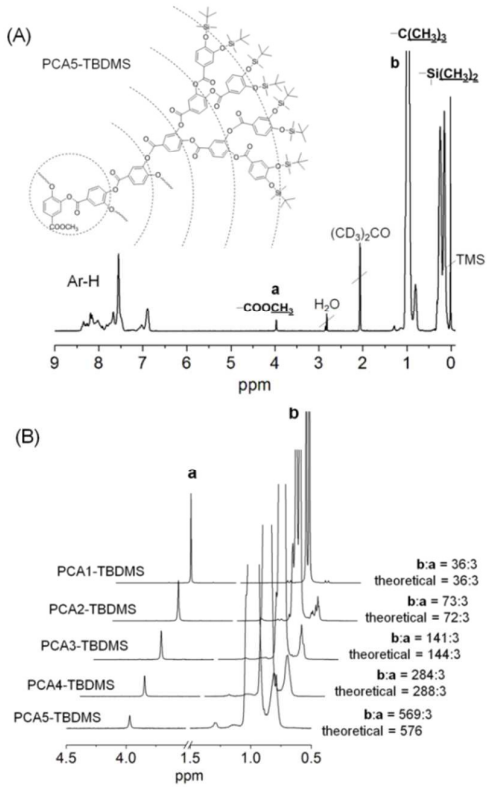

Figure 2. ^{1}H NMR spectrum of PCA5-TBDMS in $(CD_3)_2CO$ (A) and integration ratio of peak b (-Si-C(CH)$_3$, TBDMS) to peak a (-$COOCH_3$, dendrimer core) in PCAn-TBDMS (n = 1-5) ^{1}H NMR spectra (B).

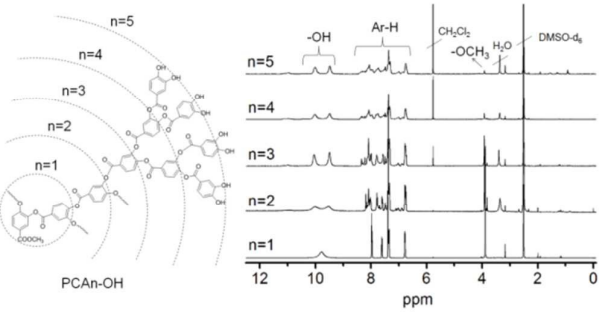

Figure 3. ^{1}H NMR spectra of PCAn-OH (n = 1, 2, 3, 4, 5) in DMSO-d_6.

The interior of PCA4-PEG consisted of benzene rings that could form strong π-π stacking interaction with the benzene ring of DOX.[17] Thus, DOX could be efficiently loaded into the dendrimer's cavity. The drug encapsulation efficiency and the drug loading content were about 99% and 15%. The size and size distribution of the PEGylated dendrimers were quantitated by dynamic light scattering (Figure 4). The average diameter of PCA4-PEG was 30 nm, with a polydispersity of 0.084. Loading DOX into PCA4-PEG did not change the nanocarriers' size. A nanocarrier between 10 and 100 nm is favorable for drug delivery that will not be cleared by renal filtration and also has reduced hepatic filtration.[29] Furthermore, these small PEGylated dendrimers may have a long blood residence time and a high rate of accumulation in the tumor tissue by passive targeting via the enhanced retention and permeability effect of tumor.[30] The zeta potential of PCA4-OH and PCA4-PEG at pH 7.4 is -11 mv and -6 mv, respectively. Loading DOX to PCA4-PEG did not

View Article Online
DOI: 10.1039/C6TB01597B

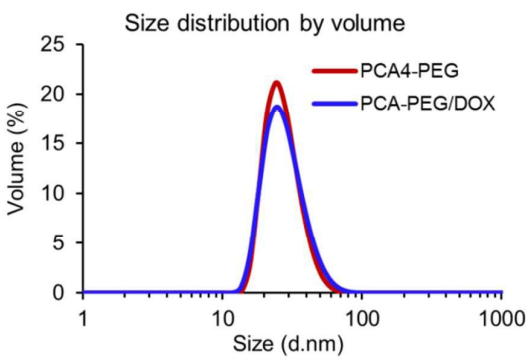

Figure 4. Size of PEGylated dendrimers measured by dynamic light scattering in HEPES buffer (0.01 M; pH 7.4).

change the surface charge of the nanocarrier. The slightly negative charged surface of nanocarrier may facilitate its accumulation and deep penetration in tumor by reducing phagocytic uptake and electrostatic adhesive interactions.[31, 32]

pH and redox-dependent drug release of PCA4-PEG/DOX

The degradation of PCA1-OH was studied and tracked by ^{1}H NMR spectra (Figure S7). When treated with dithiothreitol (DTT), a reducing agent, along with triethylamine, PA1-OH was fully degraded in three hours. The chemical shift of proton in $-OCH_3$ group gradually moved from 3.95 to 3.73 ppm in 3 hours. The chemical shift of aromatic protons also changed with culturing time. Drug release of PCA4-PEG/DOX was studied under different conditions to simulate different biological environments. As shown in Figure 5, DOX was gradually released from the dendrimer at pH 7.4 with reduced burst initial release, which may be attributed to the strong π-π stacking interaction between the dendrimer and DOX.[17] This is a great advantage over traditional nanocarriers, which are generally prone to severe burst release.[33] It is feasible and desirable to optimize the drug release profile by introducing an optimal drug-binding molecule into the nanocarrier.[34] After 48 h, about 95% of the DOX was released at pH 5.0, whereas only 38% of the DOX was released at pH 7.4. The loaded DOX was partially ionized at a lower pH, which may have reduced the binding interaction between the dendrimer and DOX, and thus triggered the rapid release of DOX at a lower pH.[17, 35] The hydrolysis of phenol ester and the destruction of PCA dendrimers at a lower pH may partly contribute to accelerated drug release. This acid-promoted drug release is favorable for anticancer drug delivery, as it may

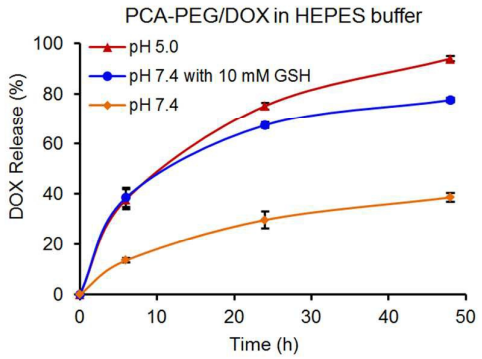

Figure 5. DOX release kinetics were determined in HEPES buffer at pH 7.4 or 5.0, or at pH 7.4 with 10 mM of GSH. Data are shown as mean ± SD (n = 3).

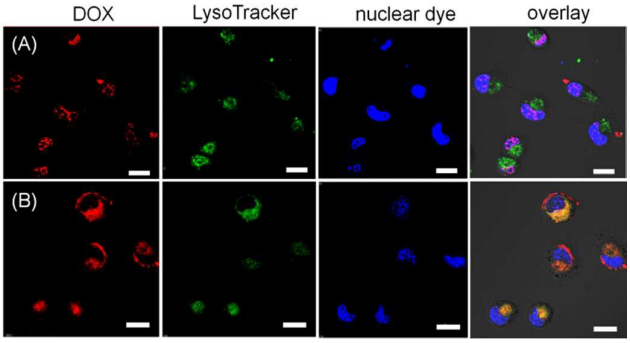

Figure 6. Intracellular localization of free DOX (A) and DOX-loaded dendrimers (B) in A549 cells was observed by CLSM after 2 h of incubation, DOX: red; lysosomal dye LysoTracker: green; nuclear dye DAPI: blue (scale bar, 20 μm).

reduce the nonspecific drug release during blood circulation (pH 7.4) and accelerate drug release in the tumor tissue (pH < 7.0) or intracellular compartments such as the endosome (pH 6.0 to 6.5) and lysosome (pH 4.5 to 5.5).[36] DOX release of PCA4-PEG/DOX was also studied in a reductive environment with 10 mM of GSH (Figure 5). Interestingly, DOX release was much faster in the presence of GSH than in its absence. About 78% of DOX was released in 48 h with the presence of 10 mM of GSH, which might be attributable to the GSH-triggered thiolysis of phenol ester in the dendrimer.[37] The GSH-dependent drug release profile of PCA4-PEG/DOX would enhance drug release in the strongly reducing intracellular environment (approximately 0.5 to 10 mM of GSH), but the release would remain slow in the blood (approximately 20 to 40 μM GSH).[38, 39] The pH and redox dual-responsive PCA4-PEG/DOX is a promising drug delivery system that can decrease side effects by reducing nonspecific drug release and meanwhile increase drug efficacy by enhancing the delivery of active drug to the target sites.[40-42]

Cellular uptake and intracellular localization of PCA4-PEG/DOX

The cellular uptake and intracellular localization of PCA4-PEG/DOX in A549 cancer cells were observed with confocal fluorescence microscopy, and free DOX was used as a control (Figure 6). PCA4-PEG/DOX or DOX was incubated with cells for 2 h, and the fluorescence of DOX appeared red. Late endosomes/lysosomes were labeled with LysoTracker, and the fluorescence appeared green. Cell nuclei were labeled with nuclear dye, and the fluorescence appeared blue. As shown in Figure 6, the overlay of PCA4-PEG/DOX and Lysotracker images shows yellow spots that indicate that PCA4-PEG/DOX was partly located in lysosomes within the 2-h incubation period. The localization of PCA4-PEG/DOX in lysosomes implies that PCA4-PEG/DOX might be taken up by endocytosis, a possible pathway for nanocarriers. When cells were incubated with free DOX, DOX was mainly found in the cell nuclei. The fluorescent intensity in cells cultured with PCA4-PEG/DOX is relatively higher than free DOX. These results demonstrate that PCA4-PEG is an efficient carrier for delivery of DOX into the cell cytoplasm, but also indicate that the internalization mechanism of the DOX-loaded dendrimer differs from that of free DOX. This finding is consistent with the reported DOX-loaded nanocarrier.[43, 44] The results also suggest that free DOX can efficiently enter cells by via passive diffusion rather than by receptor-mediated endocytosis.[45] Notably, some red fluorescence did not overlay with green fluorescence and was observed in the cytoplasm but less so in the nuclei. PCA4-PEG/DOX was internalized via an endocytosis pathway and was located first in endosome/lysosomes. The acidic

View Article Online
DOI: 10.1039/C6TB01597B

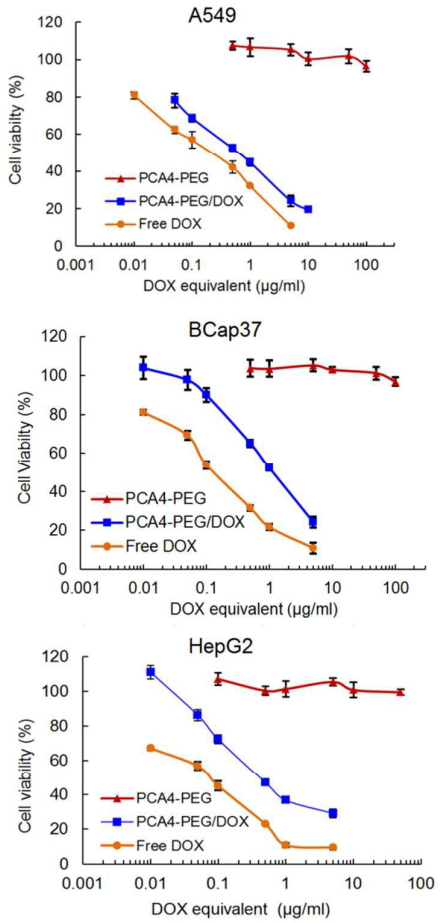

Figure 7. Cytotoxicity of PCA4-PEG, PCA4-PEG/DOX, and free DOX against A549 lung cancer cells, Bcap37 breast cancer cells, and HepG2 liver cancer cells cultured for 48 h was estimated by MTT assay. Data are presented as mean ± SD (n = 5).

environment of the endosome/lysosomes promoted the release of DOX, and some DOX was transported into cytoplasm. When cells were cultured with PCA4-PEG/DOX for 12 h (Figure S8), some DOX had already entered or was close to the nuclei, which indicates that DOX from PCA4-PEG/DOX can gradually enter nuclei to act as a DNA toxin.

***In vitro* cytotoxicity**

The *in vitro* cytotoxicity of PCA4-PEG, PCA4-PEG/DOX, and free DOX was evaluated by MTT assays against a panel of human tumor cell lines, including A549 lung cancer cells, BCap37 breast cancer cells, and HepG2 liver cancer cells. Cells were cultured with each treatment for 48 h, and the results are presented in Figure 7. Blank PCA4-PEG had no effect on cell viability within the tested concentrations as high as 100 μg/ml, which indicates that the carriers had low cytotoxicity.[46] The antitumor activity of PCA dendrimers may work by affecting the tumor microenvironment at low concentrations.[47] The IC_{50} (concentration that inhibits cell growth to 50% of control) values of DOX in PCA4-PEG/DOX to A549, BCap37, and HepG2 were 0.88, 0.94, and 0.52 μg/ml, respectively. The IC_{50} value of DOX to these cancer cells was 0.66, 0.18, and 0.16 μg/ml, respectively. Compared with DOX, PCA4-PEG/DOX showed comparable cytotoxicity to A549 cells and about three to five times less cytotoxicity to BCap37 and HepG2 cells. DOX is a DNA toxin drug that acts by stabilizing the enzyme-DNA cleavable complex leading to DNA breaks.[48] Free DOX has a much higher nuclear localization rate than PCA4-PEG/DOX as indicated by cellular distribution study (Figure 6). However, the cytotoxicity of PCA4-PEG/DOX is close to free DOX. The IC_{50} of DOX in PCA4-PEG/DOX to A549, BCap37, and HepG2, is about 1.3, 5.2 and 3.2 times of free DOX, respectively. PCA4-PEG/DOX could protect DOX from deactivation and overcome the multidrug resistance of cancer cells, but its time-consuming DOX-release and delayed delivery to nuclei lower its cytotoxicity.

***In vivo* antitumor efficacy**

The *in vivo* antitumor activity of the DOX-loaded dendrimers was evaluated with a A549 xenograft model on nude mice (eight per group) upon tail-vein injection. The antitumor efficacy of various formulations is illustrated in Figure 8A. Blank PCA4-PEG showed very low cytotoxicity in vitro, but can partially inhibit tumor growth in vivo. It has been reported that PCA can prevent tumorigenesis by reducing biomarkers of inflammation and angiogenesis[49] and can inhibit cell migration and invasion at non-cytotoxic concentrations.[47] Our finding indicates that PCA may have an antitumor effect on A549 lung tumor by acting on the tumor microenvironment. Both PCA4-PEG/DOX and free DOX (4 mg/kg)

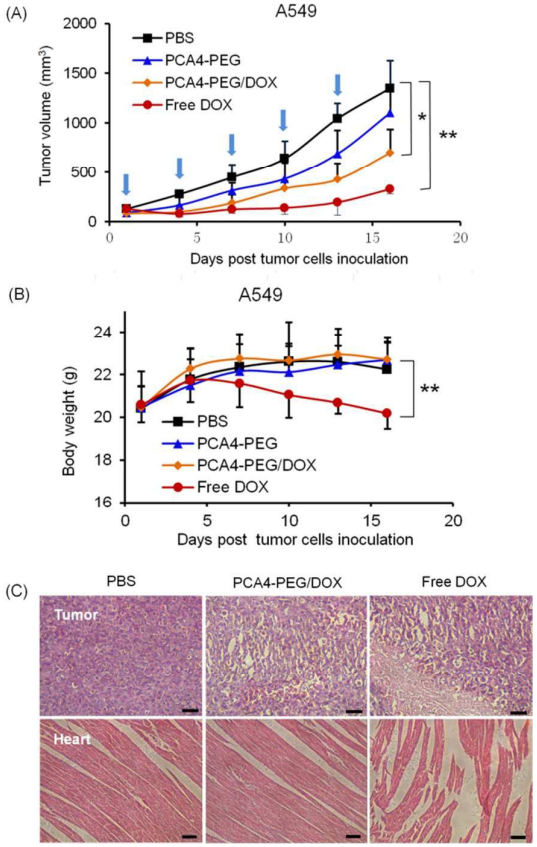

Figure 8. Antitumor activities of DOX-loaded PCA dendrimers against A549 human lung xenograft tumors. Nude mice with A549 tumors were treated with PBS, free DOX (4 mg/kg), PCA4-PEG, or PCA4-PEG/DOX (equivalent to 4 mg/kg DOX) as indicated by the arrows (q3d × 5; n = 6; data presented as average ± SE). (A) Tumor volumes of mice as function of time (* $p < 0.05$, ** $p < 0.005$). (B) Body weight of mice as function of time (** $p < 0.005$). (C) Representative histologic images of tumor and heart tissue sections (scale bar, 100 μm).

View Article Online
DOI: 10.1039/C6TB01597B

treatments effectively suppressed tumor growth compared to that seen in the control group. The TIR was calculated after the mice were sacrificed at the end of treatment. The TIR of PCA4/PEG-DOX was 48.2%, which was lower than that of free DOX (75.6%). The side effects of the treatments were preliminarily evaluated by monitoring the mice's body weight. The body weight of the mice injected with free DOX gradually decreased during treatment by about 10% of the initial weight in 12 days. The final body weight of the group treated with DOX was significantly lower than that of mice treated with PBS ($p = 0.005$). In contrast, the group treated with PCA4-PEG/DOX did not lose any obvious body weight (Figure 8B). No significant difference was found in the body weight between the groups treated with PCA4-PEG/DOX and PBS, which suggests that the encapsulation of DOX in PCA dendrimers significantly reduced the general toxicity of DOX.

The excised tumor and heart tissue was examined histologically with hematoxylin-eosin staining. As shown in Figure 8C, the tumors treated with PBS typically consisted of tightly packed tumor cells and some necrotic regions due to their rapid growth. In contrast, the tumors treated with PCA4-PEG/DOX or free DOX showed extensive nuclear shrinkage and cellularity changes in many cancer cells, which indicates that both PCA4-PEG/DOX and free DOX could induce apoptosis. Histologic analysis of heart tissue was performed to examine cardiomyocyte damage, which is the most serious side effect of DOX. Severe myocardial alterations were observed in the mice that were treated with free DOX. In contrast, the cardiac muscle fibers were clear and vivid in the mice that were treated with PCA4-PEG/DOX or PBS.

Conclusions

Dendrimers with PCA as building blocks were synthesized, characterized, and used as macromolecular drug carriers for cancer therapy. PCA in the dendrimer also served as a drug-binding molecule to facilitate drug loading and reduce burst release. The DOX-loaded dendrimer PCA-PEG/DOX exhibited pH and GSH-dual responsive drug release in vitro. PCA-PEG/DOX could be used to gradually deliver DOX to cell nuclei and showed comparable cytotoxicity to free DOX in vitro. The antitumor activity of PCA-PEG and PCA-PEG/DOX was preliminary studied. PCA-PEG showed potential antitumor activity at a noncytotoxic concentration. PCA-PEG/DOX effectively suppressed tumor growth with reduced systemic toxicity. The results show the potential of a novel dendrimer as an anticancer drug and also a sufficient nanocarrier for drug delivery.

Acknowledgements

This work was financially supported by the National Basic Research Program, Grant Number: 2014CB931900, the Fundamental Research Funds for the Central Universities (No.2016QNA4024), and the China postdoctoral science foundation (No.2013T60595).

Notes and references

1 C. C. Lee, J. A. MacKay, J. M. J. Frechet and F. C. Szoka, *Nat. Biotechnol.*, 2005, **23**, 1517-1526.
2 R. Hourani and A. Kakkar, *Macromol. Rapid Comm.*, 2010, **31**, 947-974.
3 L. M. Kaminskas, V. M. McLeod, B. D. Kelly, G. Sberna, B. J. Boyd, M. Williamson, D. J. Owen and C. J. Porter, *Nanomedicine-Uk*, 2012, **8**, 103-111.
4 J. M. Oliveira, A. J. Salgado, N. Sousa, J. F. Mano and R. L. Reis, *Prog. Polym. Sci.*, 2010, **35**, 1163-1194.
5 C. Wang, *Sci. Bull.*, 2015, **60**, 403-404.
6 E. Mohammadifar, A. N. Kharat and M. Adeli, *J. Mater. Chem. B*, 2015, **3**, 3896-3921.
7 Q. Sun, X. Ma, B. Zhang, Z. Zhou, E. Jin, Y. Shen, E. A. Van Kirk, W. J. Murdoch, M. Radosz and W. Sun, *Biomater. Sci.*, 2016, **4**, 958-969.
8 K. Jain, P. Kesharwani, U. Gupta and N. K. Jain, *Int. J. Pharm.*, 2010, **394**, 122-142.
9 H. R. Ihre, O. L. P. De Jesus, F. C. Szoka and J. M. J. Frechet, *Bioconjugate Chem.*, 2002, **13**, 443-452.
10 X. Ma, Z. Zhou, E. Jin, Q. Sun, B. Zhang, J. Tang and Y. Shen, *Macromolecules*, 2012, **46**, 37-42.
11 Z. Zhou, X. Ma, C. J. Murphy, E. Jin, Q. Sun, Y. Shen, E. A. Van Kirk and W. J. Murdoch, *Angew. Chem. Int. Ed.*, 2014, **53**, 10949-10955.
12 E. R. Gillies, E. Dy, J. M. J. Frechet and F. C. Szoka, *Mol. Pharm.*, 2005, **2**, 129-138.
13 O. L. P. De Jesus, H. R. Ihre, L. Gagne, J. M. J. Frechet and F. C. Szoka, *Bioconjugate Chem.*, 2002, **13**, 453-461.
14 X. Ma, J. Tang, Y. Shen, M. Fan, H. Tang and m. Radosz, *J. Am. Chem. Soc.*, 2009, **131**, 14795-14803.
15 T. H. Tseng, J. D. Hsu, M. H. Lo, C. Y. Chu, F. P. Chou, C. L. Huang and C. J. Wang, *Cancer Lett.*, 1998, **126**, 199-207.
16 M. C. Yin, C. C. Lin, H. C. Wu, S. M. Tsao and C. K. Hsu, *J. Agric. Food Chem.*, 2009, **57**, 6468-6473.
17 T. Yamanoi, Y. Oda, K. Katsuraya, T. Inazu and K. Hattori, *Bioorgan. Med. Chem.*, 2016, **24**, 635-642.
18 O. Swiech, P. Dutkiewicz, K. Wojciuk, K. Chmurski, M. Kruszewski and R. Bilewicz, *J. Phys. Chem. B*, 2013, **117**, 13444-13450.
19 W. S. Li, K. S. Kim, D. L. Jiang, H. Tanaka, T. Kawai, J. H. Kwon, D. Kim and T. Aida, *J. Am. Chem. Soc.*, 2006, **128**, 10527-10532.
20 Y. Ren, K. Himmeldirk and X. Chen, *J. Med. Chem.*, 2006, **49**, 2829-2837.
21 A. Alam, Y. Takaguchi, H. Ito, T. Yoshida and S. Tsuboi, *Tetrahedron*, 2005, **61**, 1909-1918.
22 C. J. Hawker and J. M. J. Frechet, *J. Am. Chem. Soc.*, 1990, **112**, 7638-7647.
23 D. A. Tomalia, A. M. Naylor and W. A. Goddard, *Angew. Chem. Int. Ed.*, 1990, **29**, 138-175.
24 T. B. T. Nguyen, T. T. C. Nguyen, H. C. Tran, C. K. Nguyen and N. Q. Tran, *Int. J. Polym. Anal. Ch.*, 2015, **20**, 57-68.
25 K. F. Medzihradszky, J. M. Campbell, M. A. Baldwin, A. M. Falick, P. Juhasz, M. L. Vestal and A. L. Burlingame, *Anal. Chem.*, 2000, **72**, 552-558.
26 M. T. Peracchia, E. Fattal, D. Desmaele, M. Besnard, J. P. Noel, J. M. Gomis, M. Appel, J. d'Angelo and P. Couvreur, *J. Controlled Release*, 1999, **60**, 121-128.
27 Z. Zhou, J. Tang, Q. Sun, W. J. Murdoch and Y. Shen, *J. Mater. Chem. B*, 2015, **3**, 7594-7603.
28 F. M. Veronese and G. Pasut, *Drug Discov. Today*, 2005, **10**, 1451-1458.
29 F. Alexis, E. Pridgen, L. K. Molnar and O. C. Farokhzad, *Mol. Pharm.*, 2008, **5**, 505-515.
30 H. Maeda, *Adv. Drug Deliv. Rev.*, 2015, **91**, 3-6.
31 K. Xiao, Y. Li, J. Luo, J. S. Lee, W. Xiao, A. M. Gonik, R. G. Agarwal and K. S. Lam, *Biomaterials*, 2011, **32**, 3435-3446.
32 J. Bugno, H.-J. Hsu, R. M. Pearson, H. Noh and S. Hong, *Mol. Pharm.*, 2016, DOI: 10.1021/acs.molpharmaceut.5b00946.

View Article Online
DOI: 10.1039/C6TB01597B

33 G. R. Tan, S. S. Feng and D. T. Leong, *Biomaterials*, 2014, **35**, 3044-3051.
34 C. Y. Shi, D. D. Guo, K. Xiao, X. Wang, L. L. Wang and J. T. Luo, *Nat. Commun.*, 2015, **6**.
35 Y. H. Bae, D. Kim, E. S. Lee, K. T. Oh and Z. G. Gao, *Small*, 2008, **4**, 2043-2050.
36 Z. Zhou, W. J. Murdoch and Y. Shen, *Polymer*, 2015, **76**, 150-158.
37 J. Wang, X. Sun, W. Mao, W. Sun, J. Tang, M. Sui, Y. Shen and Z. Gu, *Adv. Mater.*, 2013, **25**, 3670-3676.
38 D. H. Yu, G. Y. Zou, X. J. Cui, Z. W. Mao, I. Estrela-Lopis, E. Donath and C. Y. Gao, *J. Mater. Chem. B*, 2015, **3**, 8865-8873.
39 Z. Zhou, Y. Shen, J. Tang, M. Fan, E. A. Van Kirk, W. J. Murdoch and M. Radosz, *Adv. Funct. Mater.*, 2009, **19**, 3580-3589.
40 S. Mura, J. Nicolas and P. Couvreur, *Nat. Mater.*, 2013, **12**, 991-1003.
41 W. R. Cheng, J. N. Kumar, Y. Zhang and Y. Liu, *Biomater. Sci.*, 2015, **3**, 597-607.
42 Y. Zhang, C. S. Xiao, M. Q. Li, J. X. Ding, C. L. He, X. L. Zhuang and X. S. Chen, *Polym. Chem.*, 2014, **5**, 2801-2808.
43 X. T. Shuai, H. Ai, N. Nasongkla, S. Kim and J. M. Gao, *J. Control. Release*, 2004, **98**, 415-426.
44 Z. Zhou, W. J. Murdoch and Y. Shen, *J. Polym. Sci. Polym. Chem.*, 2016, **54**, 507-515.
45 Z. G. Xu, K. L. Zhang, C. L. Hou, D. D. Wang, X. Y. Liu, X. J. Guan, X. Y. Zhang and H. X. Zhang, *J. Mater. Chem. B*, 2014, **2**, 3433-3437.
46 E. C. H. Yip, A. S. L. Chan, H. Pang, Y. K. Tam and Y. H. Wong, *Cell Biol. Toxicol.*, 2006, **22**, 293-302.
47 H. H. Lin, J. H. Chen, F. P. Chou and C. J. Wang, *Br. J. Pharmacol.*, 2011, **162**, 237-254.
48 L. H. Hurley, *Nat. Rev. Cancer*, 2002, **2**, 188-200.
49 D. S. Peiffer, N. P. Zimmerman, L. S. Wang, B. W. S. Ransom, S. G. Carmella, C. T. Kuo, J. Siddiqui, J. H. Chen, K. Oshima, Y. W. Huang, S. S. Hecht and G. D. Stoner, *Cancer Prev. Res.*, 2014, **7**, 574-584.